

## Photoinduced Electron Transfer in Nucleic Acid Molten Salts

Anthony M. Leone, Matthew K. Brennaman, Jennifer D. Tibodeau, John M. Papanikolas,\*  
Royce W. Murray,\* and H. Holden Thorp\*

Department of Chemistry, University of North Carolina at Chapel Hill,  
Chapel Hill, North Carolina 27599-3290

Received: December 12, 2002; In Final Form: April 22, 2003

Molten salts of  $\text{Ni}(\text{bpy}_{350})_3^{2+}$  and single stranded oligonucleotides were prepared ( $\text{bpy}_{350} = 4,4'-(\text{CH}_3(\text{OCH}_2\text{CH}_2)_{7.24}\text{OCO})_2-2,2'$ -bipyridine). Photoinduced electron transfer was observed between small amounts of  $\text{Ru}(\text{bpz})_3^{2+*}$  ( $E^{2+*/1+} = 1.35$  V vs SCE,  $\text{bpz} = 2,2'$ -bipyrazine) added to the melt and guanine in the nucleic acid, by measuring the emission lifetime of the ruthenium complex in melts containing varying amounts of guanine-containing nucleic acid. Electrochemically determined diffusion coefficients in these media were  $< 1 \times 10^{-11}$   $\text{cm}^2/\text{s}$ , showing that the  $\text{Ru}(\text{bpz})_3^{2+*}$  diffuses less than  $0.4$  Å during the measured excited-state lifetime. A linear relationship was observed between the fraction of  $\text{Ru}(\text{bpz})_3^{2+*}$  that was quenched (calculated as  $(\tau^\circ - \tau)/\tau$ ) and the mole fraction of guanine-containing oligonucleotides. This relationship supports a quenching mechanism that does not involve diffusion of the ruthenium complex. The average electron-transfer rate constant at full guanine loading was  $7 \times 10^6$   $\text{s}^{-1}$ , which implies an average electron-transfer distance of  $12.5$  Å (center-to-center).

The mobility of electrons in thin films on electrode surfaces is of interest in the development of electrochemical devices and in illuminating the general principles of electron transfer in macromolecular structures.<sup>1</sup> Early efforts involving covalently attached metal centers electropolymerized on solid electrodes<sup>2</sup> or tethered to self-assembled monolayers<sup>3</sup> revealed a number of fundamental principles regarding electron transfer to solid electrodes and among redox-active sites in thin films. Additional insights have been gained by preparing ionic liquids (molten salts or just “melts”) where one ionic partner is decorated with polyether tails.<sup>4–7</sup> These materials comprise authentic solutions and—as thin films on electrodes—provide simple electrochemical responses. The slow diffusion in these molten materials and the ability to perform analysis with microelectrodes in the absence of any added solvent component enable the observation of electron transfers between the redox sites in the ionic liquid. In addition to the insights into fundamental electron transfer provided by these systems, the physical chemistry of ionic liquids and molten salts is an area of particularly intense interest.<sup>8</sup>

Self-assembled monolayers and electropolymerized films have similarly been used to study electron-transfer reactions where DNA is present on an electrode surface or is one of the redox partners in a surface-bound electrochemical reaction.<sup>9,10</sup> We have developed new methods for preparing thin films of DNA on electrodes involving highly viscous, ionic liquids made from DNA (anions) and metal complex cations with ligands that are decorated with polyether tails,<sup>11</sup> such as  $\text{bpy}_{350}$  in Figure 1. Extremely slow physical diffusion of the polyether-decorated metal complex cation in these phases can be determined directly by electrochemical analysis<sup>7,11,12</sup> of the neat melts to give diffusion coefficient values where  $D_{\text{PHYS}} < 10^{-11}$   $\text{cm}^2/\text{s}$ . The DNA concentrations attainable in these media ( $0.65$  M) are quite high, and the polyether tails allow maintenance of double-helical structure when melts are formed using duplex DNA. The electrochemical studies show that charge can be transported

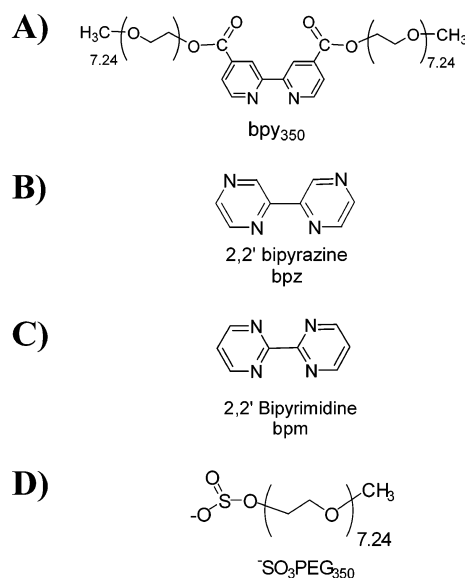


**Figure 1.** Structures of (A)  $\text{bpy}_{350}$ , (B) 2,2' bipyrazine (bpz), (C) 2,2' bipyrimidine (bpm), and (D)  $^{-}\text{SO}_3\text{PEG}_{350}$ .

through the melts by metal-centered electron hopping, when the intrinsic self-exchange reaction of the participating metal complex is efficient. Ground-state electron transfer between metal centers and the DNA becomes apparent as catalytic currents, provided the included metal complex is a sufficiently powerful oxidant to remove an electron from the guanine nucleobase (approximately  $1.05$  V vs SCE).

We report here on photochemical studies of metal complexes such as  $\text{Ru}(\text{bpz})_3^{2+}$  (see Figure 1 for ligand structure) in DNA molten salts. On the basis of the known photochemical properties of these complexes<sup>13–15</sup> and recent studies on the one-electron oxidation of guanine,<sup>10,16,17</sup> we suspected that oxidation of guanine in DNA by excited states of ruthenium polypyridyl complexes would lead to emission quenching that could be

followed by time-resolved emission spectroscopy. Consistent with previous studies in dilute solution, the parent  $\text{Ru}(\text{bpy})_3^{2+}$  complex is not a sufficiently powerful excited-state oxidant to abstract electrons from guanine ( $\text{bpy} = 2,2'$ -bipyridine);<sup>9</sup> however, derivatives that are more potent excited-state oxidants undergo emission quenching by guanine in the molten salts. The extent of quenching can be analyzed in terms of the restricted diffusion of the redox partners. These studies provide further insight into the physical properties of high-viscosity ionic liquids.

## Experimental Section

Millipore ultrapure water was used for all experiments. All reagents were purchased from Sigma Aldrich unless otherwise noted. 2,2'-Bipyrimidine (bpm) was purchased from Lancaster Synthesis and twice recrystallized from ether before use. Oligonucleotides were obtained from MWG-Biotech, Inc. The sequence of oligonucleotide **1** is 5'-GAT GAA GTG TGA TGT AGA AGA TGT G, and the sequence of **2** is 5'-CAC ATC TTC TAC ATC ACA CTT CAT C. Concentrations were determined using the following molar absorptivities:  $\text{Ni}(\text{bpy}_{350})_3^{2+}$ ,  $\epsilon_{327} = 27\,800\text{ M}^{-1}\text{ cm}^{-1}$ ;  $\text{Ru}(\text{bpy})_3^{2+}$ ,  $\epsilon_{452} = 14\,000\text{ M}^{-1}\text{ cm}^{-1}$ ;  $\text{Ru}(\text{bpz})_3^{2+}$ ,  $\epsilon_{440} = 13\,000\text{ M}^{-1}\text{ cm}^{-1}$ ;  $\text{Ru}(\text{bpm})_3^{2+}$ ,  $\epsilon_{454} = 8600\text{ M}^{-1}\text{ cm}^{-1}$ ; oligo **1**,  $\epsilon_{262} = 12\,075\text{ M}^{-1}\text{ cm}^{-1}$ ; oligo **2**,  $\epsilon_{258} = 10\,050\text{ M}^{-1}\text{ cm}^{-1}$ . Absorption measurements were performed using a Cary300Bio UV-vis Spectrophotometer. Steady-state luminescence measurements were performed on a Spex Fluoromax spectrofluorimeter.

**Synthesis.** 2,2'-Bipyrazine (bpz) was prepared by the procedure of Lafferty and Case.<sup>18</sup> The complexes  $\text{Ru}(\text{bpz})_3\text{Cl}_2$  and  $\text{Ru}(\text{bpm})_3\text{Cl}_2$  were prepared according to Rillema and Meyer.<sup>14</sup> Synthesis of  $\text{Ni}(\text{bpy}_{350})_3(\text{ClO}_4)_2$  was performed as previously described.<sup>5</sup> Synthesis of  $\text{NaSO}_3\text{MePeg}_{350}$  was performed as described previously,<sup>19</sup> and  $\text{Ru}(\text{bpz})_3(\text{SO}_3\text{MePeg}_{350})_2$ ,  $\text{Ru}(\text{bpm})_3(\text{SO}_3\text{MePeg}_{350})_2$ , and  $\text{Ru}(\text{bpy})_3(\text{SO}_3\text{MePeg}_{350})_2$  were synthesized by the methods of Ritchie and Murray.<sup>20</sup> Syntheses of  $\text{Ni}(\text{bpy}_{350})_3\cdot\mathbf{1}$  and  $\text{Ni}(\text{bpy}_{350})_3\cdot\mathbf{2}$ , where the metal complex is a stoichiometric counterion of the oligonucleotide phosphates, were achieved through dialysis, as described previously for  $\text{Co}(\text{bpy}_{350})_3\cdot\text{DNA}$ , with slight modification as follows.<sup>11</sup> Aqueous solutions containing 1.2 equiv of  $\text{Ni}(\text{bpy}_{350})_3(\text{ClO}_4)_2$  and 2 equiv of nucleotide were mixed in a 1000 MWCO dialysis tubing. The dialysis was intended to remove the perchlorate counterions, the excess metal complex  $\text{Ni}(\text{bpy}_{350})_3(\text{ClO}_4)_2$ , and the native sodium cations of the nucleotide. The tubing was placed in a 1-L water reservoir for 4 days at 4 °C. The water was changed every 24 h. The quantity of the  $\text{Ni}(\text{bpy}_{350})_3(\text{ClO}_4)_2$  exchanged out of the bag was monitored spectrophotometrically by measuring the reservoir absorbance at 327 nm using the determined extinction coefficient ( $27\,800\text{ M}^{-1}\text{ cm}^{-1}$ ). The  $\text{Ni}(\text{bpy}_{350})_3^{2+}$  complex is exchanged slowly enough that the maximum quantity of sodium perchlorate exits before equilibrium is reached. Equilibrium is when the Ni complex ceases to enter the reservoir because there are no longer any perchlorate counterions to accompany it in permeation.

**Gel Electrophoresis.** Radiolabeled ATP was purchased from New England Nuclear. T4 Kinase was purchased from either Promega or New England Biolabs. Oligonucleotides were synthesized by the Lineberger Comprehensive Cancer Center Nucleic Acids Core facility. Photolysis was performed with a 300 W Hg lamp (Oriel) with a 350 nm cutoff filter. Final concentrations were 50  $\mu\text{M}$  HT DNA, 12.5 fM radiolabeled oligonucleotide, 2.5  $\mu\text{M}$   $\text{Ru}(\text{bpz})_3^{2+}$ , and 500 mM  $\text{NaPi}$ , pH 7. The irradiation time was 1 min, and the total volume was 80

$\mu\text{L}$ . Samples were precipitated with sodium acetate and ethanol, subjected to alkaline treatment with piperidine for 30 min at 90 °C, redissolved in 0.5X TBE buffer with orange G and xylene cyanole in 80% formamide, and loaded onto a denaturing (7 M urea) 20% acrylamide gel. Gels were visualized using a Molecular Dynamics Phosphorimager and ImageQuant software.

### Variation of Guanine Concentration in Molten Salts.

Following dialysis, the solutions of  $\text{Ni}(\text{bpy}_{350})_3\cdot\mathbf{1}$  or  $\text{Ni}(\text{bpy}_{350})_3\cdot\mathbf{2}$  were removed, and individual concentrations were determined by optical absorption using  $\epsilon = 27\,800\text{ M}^{-1}\text{ cm}^{-1}$  at 327 nm. From these solutions, mixtures of  $\text{Ni}(\text{bpy}_{350})_3\cdot\mathbf{1}$  and  $\text{Ni}(\text{bpy}_{350})_3\cdot\mathbf{2}$  with  $\text{Ru}(\text{bpz})_3^{2+}$  were obtained by adding the following:  $[\text{Ni}(\text{bpy}_{350})_3\cdot\mathbf{2} + 0.14\text{Ni}(\text{bpy}_{350})_3\cdot\mathbf{1}]$ ,  $[\text{Ni}(\text{bpy}_{350})_3\cdot\mathbf{2} + 0.60\text{Ni}(\text{bpy}_{350})_3\cdot\mathbf{1}]$ ,  $[\text{Ni}(\text{bpy}_{350})_3\cdot\mathbf{2} + 3\text{Ni}(\text{bpy}_{350})_3\cdot\mathbf{1}]$ , and  $[\text{Ni}(\text{bpy}_{350})_3\cdot\mathbf{2} + 7\text{Ni}(\text{bpy}_{350})_3\cdot\mathbf{1}]$ . To each mixture, 1 equiv of the  $\text{Ru}(\text{bpz})_3(\text{SO}_3\text{MePeg}_{350})_2$  was added for 10 equiv of the total  $\text{Ni}(\text{bpy}_{350})_3^{2+}$  concentration. This produced solutions of composition 1  $\text{Ru}(\text{bpz})_3^{2+}$ :10  $\text{Ni}(\text{bpy}_{350})_3^{2+}$ :20 nucleotides that varied only in their guanine content. Solutions were reduced in volume to 10  $\mu\text{L}$  and cast on quartz slides that were placed in a vacuum desiccator with anhydrous  $\text{CaSO}_4$  for 6 h followed by drying at  $10^{-3}$  Torr for 12 h. Samples containing the strong photooxidant  $\text{Ru}(\text{bpz})_3^{2+}$  were always shielded from light with aluminum foil prior to analysis. Density of dry molten salts determined by pycnometry ( $d = 1.124\text{ g/mL}$ ) gives  $[\text{Ni}(\text{bpy}_{350})_3^{2+}] = 0.327\text{ M}$ .

**Time-Resolved Emission.** All emission decay lifetimes were monitored using time-correlated single photon counting. The apparatus consists of a commercially available argon ion laser whose continuous output was used to pump a mode-locked Ti:sapphire laser. The Ti:sapphire laser output was frequency-doubled to 423 nm using a BBO crystal to produce  $\sim 1$  ps pulses with a pulse energy of  $\sim 0.26\text{ nJ/pulse}$  at 76 MHz. The repetition rate was selected to be roughly 5 times the natural lifetime of the sample using an acousto-optic modulator. Luminescence lifetime data were collected using a time-correlated single photon counting instrument described elsewhere.<sup>21</sup>

## Results and Discussion

The complex  $\text{Ru}(\text{bpz})_3^{2+}$  (Figure 1) is a strong excited-state oxidant ( $E^{(2+/1+)} \sim 1.35\text{ V vs SCE}$ )<sup>14</sup> and is capable of extracting electrons from numerous small molecules in dilute aqueous solution upon photoexcitation.<sup>15,22</sup> Quenching of the  $\text{Ru}(\text{bpz})_3^{2+}$  emission at 610 nm in dilute aqueous solution occurs for example upon addition of 2'-deoxyguanosine-5'-monophosphate (dGMP) or poly(d[GC]) $\cdot$ poly(d[GC]) and follows Stern-Volmer kinetics to give rate constants of  $1.6 \times 10^9$  and  $2.2 \times 10^9\text{ M}^{-1}\text{ s}^{-1}$ , respectively. The Stern-Volmer plots for dGMP and poly(d[GC]) $\cdot$ poly(d[GC]) are shown in Figure 2. The  $\text{Ru}(\text{bpz})_3^{2+}$  emission is unaffected by the addition of a saturated solution of 2'-deoxycytosine-5'-monophosphate (dCMP) or thymidine-5'-monophosphate (TMP). Further, radiolabeled nucleotides photolyzed with visible light in the presence of the  $\text{Ru}(\text{bpz})_3^{2+}$  show piperidine-labile, guanine-specific cleavage as visualized by gel electrophoresis (Figure 3). These experiments strongly implicate electron transfer from guanine to  $\text{Ru}(\text{bpz})_3^{2+}$  as the quenching mechanism.

We next prepared DNA melts that contained  $\text{Ru}(\text{bpz})_3^{2+}$  to determine whether the guanine electron transfer could be realized in the molten salts. Nucleic acid melts were prepared by extensive dialysis of  $\text{Ni}(\text{bpy}_{350})_3(\text{ClO}_4)_2$  ( $\text{bpy}_{350} = 4,4'$ -( $\text{CH}_3(\text{OCH}_2\text{CH}_2)_{7.24}\text{OCO}$ )<sub>2</sub>-2,2'-bipyridine) with either 5'-GAT GAA GTG TGA TGT AGA AGA TGT G-3' (**1**) or 5'-CAC ATC TTC TAC ATC ACA CTT CAT C-3' (**2**) to produce a

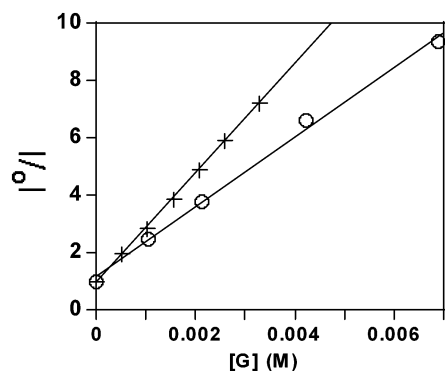


**Figure 2.** Stern–Volmer plot of  $I^\circ/I$  vs [quencher] for 5  $\mu\text{M}$   $\text{Ru}(\text{bpz})_3\text{Cl}_2$  in the presence of  $\text{poly}(\text{d}[\text{GC}])\cdot\text{poly}(\text{d}[\text{GC}])$  in 0.1 M pH 7 sodium phosphate buffer (+) and dGMP in 0.5 M pH 7 sodium phosphate buffer (O).

guanine-containing DNA melt ( $\text{Ni}(\text{bpy}_{350})_3\cdot\mathbf{1}$ ) and a DNA melt with no guanines ( $\text{Ni}(\text{bpy}_{350})_3\cdot\mathbf{2}$ ). Although **1** and **2** are complementary, native gel electrophoresis shows that hybridization does not occur under our conditions. The complex  $\text{Ru}(\text{bpz})_3(\text{SO}_3\text{PEG}_{350})_2$  was added to these melts at a concentration of 1 Ru:10 Ni:20 nucleotides (structure of  $\text{SO}_3\text{PEG}_{350}$  shown in Figure 1). The general structure of the melts is illustrated in Scheme 1. ( $\text{Ni}(\text{bpy}_{350})_3\cdot\mathbf{1}$ ) and ( $\text{Ni}(\text{bpy}_{350})_3\cdot\mathbf{2}$ ), each containing the added  $\text{Ru}(\text{bpz})_3(\text{SO}_3\text{PEG}_{350})_2$ , were combined to generate a series of melts in which the concentration of the guanine sites is varied while maintaining a constant overall proportion of nucleotides.

The emission decay of  $\text{Ru}(\text{bpz})_3^{2+*}$  in the melts was determined by time-correlated single photon counting. The measured lifetimes decreased with increasing guanine content (Table 1). A biexponential was required to fit the emission decay in the molten salt, producing the fast ( $\tau_f$ ) and slow ( $\tau_s$ ) components shown in Table 1. Although the emission decay of  $\text{Ru}(\text{bpz})_3^{2+*}$  in dilute solution is monoexponential,<sup>14</sup> the observation of a biexponential decay in the molten salt is not surprising, since simple complexes such as  $\text{Ru}(\text{phen})_3^{2+}$  exhibit biexponential decays in the presence of DNA in dilute aqueous solution.<sup>23</sup> Further, we have observed that even simple complexes based on  $\text{Ru}(\text{bpy})_3^{2+}$  exhibit biexponential decays in the molten salt environment. Both the fast and slow time components display similar extents of quenching. Weighted averages  $\langle\tau\rangle$  were determined for each fit where  $\langle\tau\rangle = \% \tau_f(\tau_f) + \% \tau_s(\tau_s)$ , and the percent contribution of each time component was determined as  $(a_i\tau_i)/(a_i\tau_i + a_j\tau_j)$ , where  $a_i$  are the pre-exponential factors for each component. As expected, the complexes  $\text{Ru}(\text{bpy})_3^{2+}$  and  $\text{Ru}(\text{bpm})_3^{2+}$  ( $\text{bpm} = 2,2'$ -bipyrimidine), which are both less potent excited-state oxidants<sup>14</sup> than  $\text{Ru}(\text{bpz})_3^{2+}$ , gave emission lifetimes that were the same in either  $\text{Ni}(\text{bpy}_{350})_3\cdot\mathbf{1}$  or  $\text{Ni}(\text{bpy}_{350})_3\cdot\mathbf{2}$ , further implicating an electron-transfer deactivation mechanism for the  $\text{Ru}(\text{bpz})_3^{2+}$  case.

The quenching of  $\text{Ru}(\text{bpz})_3^{2+*}$  in the melt did not follow Stern–Volmer kinetics for either time component (Supporting Information). Using a value for the diffusion coefficient for  $\text{Ru}(\text{bpz})_3^{2+}$  of  $D_{\text{PHYS}} = 1 \times 10^{-11} \text{ cm}^2/\text{s}$  suggests that the complex diffuses less than 0.4 Å (calculated as  $(2D_{\text{PHYS}}t)^{1/2}$ ) within the observed lifetimes.<sup>24</sup> Thus, diffusion-based quenching is not expected. The dependence of the lifetime on guanine concentration must therefore be analyzed using a model designed for quenching in rigid solutions.<sup>25,26</sup> A simple sphere-of-action or Perrin model<sup>27</sup> states that donor and acceptor only react if within a critical quenching volume, and quenching occurs with unit efficiency when donor and acceptor are within that critical quenching volume or sphere of action. This model can be

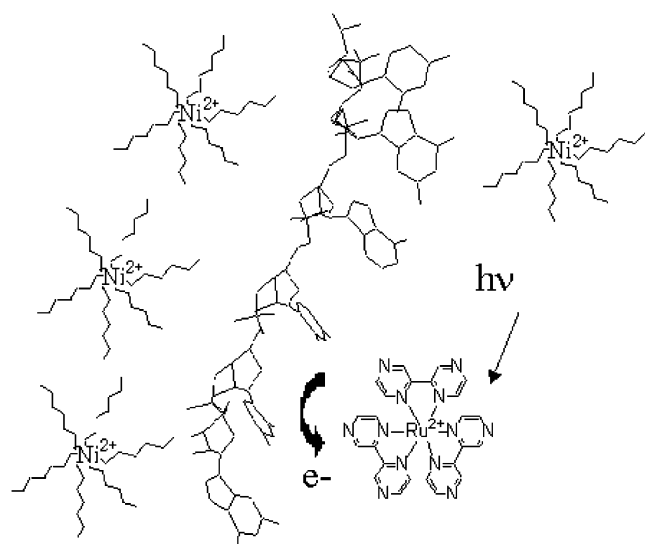


**Figure 3.** Phosphorimage of a denaturing polyacrylamide gel showing the results of photolytic cleavage of **1** (lanes 1–3) and **2** (lanes 4–5): lane 1, Maxam–Gilbert G sequencing lane for **1**; lane 2, 50  $\mu\text{M}$  HT DNA, 12.5 fM **1**, and 500 mM  $\text{NaPi}$ , no  $\text{Ru}(\text{bpz})_3^{3+}$ ; lane 3, 50  $\mu\text{M}$  HT DNA, 12.5 fM **1**, 2.5  $\mu\text{M}$   $\text{Ru}(\text{bpz})_3^{3+}$ , and 500 mM  $\text{NaPi}$ ; lane 4, 50  $\mu\text{M}$  HT DNA, 12.5 fM **2**, and 500 mM  $\text{NaPi}$ , no  $\text{Ru}(\text{bpz})_3^{3+}$ ; lane 5, 50  $\mu\text{M}$  HT DNA, 12.5 fM **2**, 2.5  $\mu\text{M}$   $\text{Ru}(\text{bpz})_3^{3+}$ , and 500 mM  $\text{NaPi}$ . Results show that guanines are photolytically cleaved by the excited-state ruthenium complex (lane 3) while cleavage at adenine sites is much lower (lane 5). Note that the sequences used here are different from **1** and **2** by the addition of the sequence GTA TA at the 3' end of **1** and TAT AC at the 5' end of **2** to facilitate visualizing the cleavage reaction by electrophoresis.

expressed quantitatively as

$$\tau^\circ/\tau = \exp(NV_c[Q]) \quad (1)$$

where  $\tau^\circ$  is the luminescence lifetime in the absence of quencher,  $\tau$  is the luminescence lifetime in the presence of quencher at concentration  $[Q]$ ,  $N$  is  $6.02 \times 10^{23}$ , and  $V_c$  is the critical quenching volume. For quenching following the Perrin formulation, a plot of  $\ln(\tau^\circ/\tau)$  should be linear with y-intercept of 0, and the slope contains the critical volume component. This approach was quite successful in early studies of photoinduced electron-transfer involving  $\text{Ru}(\text{bpy})_3^{2+}$  ( $\text{bpy} = 2,2'$ -bipyridine) and small molecule quenchers<sup>26</sup> in rigid solution. When the lifetimes for  $\text{Ru}(\text{bpz})_3^{2+}$  are analyzed with this model, the plot exhibits significant upward curvature (Figure 4A). The ex-

**SCHEME 1: Cartoon Depicting Electron Transfer Quenching of Photoexcited Ru(bpz)<sub>3</sub><sup>2+</sup> by Ni(bpy<sub>350</sub>)<sub>3</sub>•1.**


tremely short lifetimes of Ru(bpz)<sub>3</sub><sup>2+</sup>\* in melt mixtures containing large amounts of Ni(bpy<sub>350</sub>)<sub>3</sub>•1 imply that most of the ruthenium excited states are quenched at 100% guanine.

The sphere-of-action model<sup>27</sup> applied in Figure 4A assumes random distribution of the reactants and does not account for localization of Ru(bpz)<sub>3</sub><sup>2+</sup> along the DNA backbone. We therefore sought to analyze the fraction of excited states quenched, which could be calculated as  $(\tau^0 - \tau)/\tau^0$ . Figure 4B shows that there is a linear relationship between this fraction and the fraction of guanine-containing oligonucleotides. This relationship indicates that Ru(bpz)<sub>3</sub><sup>2+</sup> nearly always electrostatically associates with an oligonucleotide rather than randomly distributing itself throughout the melt volume. Oligonucleotide **1** was designed such that, for any Ru(bpz)<sub>3</sub><sup>2+</sup> electrostatically associated with phosphate, that phosphate either is part of a guanine nucleotide or is adjacent to a guanine nucleotide. Molecular models suggest that Ru(bpz)<sub>3</sub><sup>2+</sup> bound to a guanine nucleotide is 10–13 Å from a guanine (Supporting Information). Thus, as the mole fraction of **1** is increased, the mole fraction of Ru(bpz)<sub>3</sub><sup>2+</sup> (and of its excited states) bound to **1** (and, hence, undergoing electron transfer) increases linearly.

The average lifetime of 148 ns for the sample with 100% **1** gives an electron-transfer rate of  $7 \times 10^6 \text{ s}^{-1}$  for reaction of bound Ru(bpz)<sub>3</sub><sup>2+</sup>\* with guanine in the oligonucleotide. Steenken<sup>17</sup> has determined that the potential for one-electron oxidation of guanine is 1.34 V and that for the one-electron/one-proton oxidation of guanine is 1.05 V vs SCE. The fact that Ru(bpm)<sub>3</sub><sup>2+</sup>•/1<sup>+</sup> ( $E^\circ = 1.05 \text{ V}$  vs SCE) oxidizes guanine in

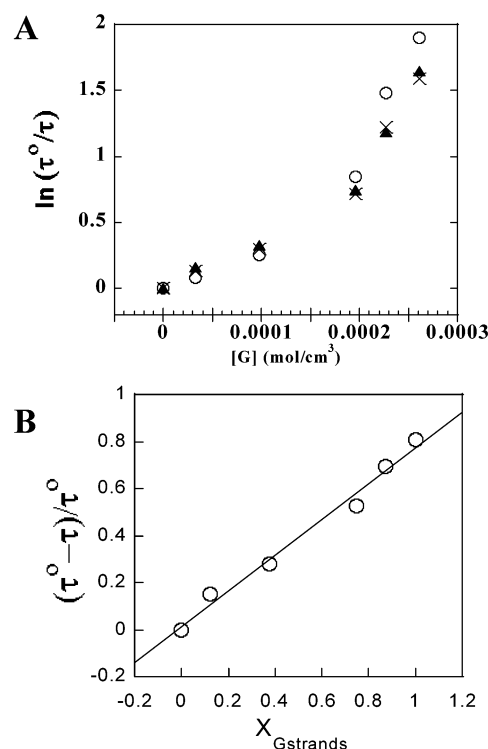


**Figure 4.** (A) Plot of  $\ln(\tau^0/\tau)$  for the Ru(bpz)<sub>3</sub><sup>2+</sup> emission as a function of guanine concentration in Ni(bpy<sub>350</sub>)<sub>3</sub><sup>2+</sup> molten salts for the fast component (x) and the slow component (○), and (▲) the weighted average of the biexponential fits. (B) Fraction of Ru(bpz)<sub>3</sub><sup>2+</sup> quenched vs mole fraction of G strands in Ni(bpy<sub>350</sub>)<sub>3</sub> DNA molten salts (same data as in part A, only weighted average shown). The concentration of guanine-containing strands was altered by varying the relative proportion of Ni(bpy<sub>350</sub>)<sub>3</sub>•1 and Ni(bpy<sub>350</sub>)<sub>3</sub>•2 while maintaining the total nucleotide concentration at 0.65 M, [Ru(bpz)<sub>3</sub><sup>2+</sup>] = 0.033 M, and [Ni(bpy<sub>350</sub>)<sub>3</sub><sup>2+</sup>] = 0.33 M.

aqueous solution (Stern–Volmer plot provided in the Supporting Information) but is not quenched in the anhydrous melt environment suggests that the electron transfer in the melt does not involve rapid deprotonation, which is expected, since there is no base to accept the proton from guanine following oxidation. The other nucleobases are apparently not sufficiently basic to accept a proton under these conditions. Use of the one-electron potential gives a driving force for the reaction of guanine with Ru(bpz)<sub>3</sub><sup>2+</sup>\* close to 0 eV.

We next sought to assess the effect of the intervening medium on the electron-transfer reaction in the novel DNA molten salt environment. To perform this analysis, we assume that the electron-transfer rate is described<sup>28</sup> by  $k = 10^{13} \text{ s}^{-1} \exp[-(\Delta G + \lambda)^2/4\lambda kT] \exp(-\beta(r - r^0))$ , where  $r$  is the average electron-transfer distance,  $r^0$  is the distance of closest approach of

**TABLE 1: Emission Lifetimes for Ruthenium Complexes in Ni(bpy<sub>350</sub>)<sub>3</sub>•DNA Melts**

material <sup>a</sup>	$\tau_f^b$	$\tau_s^b$	$\langle \tau \rangle^c$ (ns)	[guanine] (M)
Ru(bpm) <sub>3</sub> <sup>2+</sup> in Ni(bpy <sub>350</sub> ) <sub>3</sub> •1	66 ns (16%)	193 ns (84%)	172	0.2616
Ru(bpm) <sub>3</sub> <sup>2+</sup> in Ni(bpy <sub>350</sub> ) <sub>3</sub> •2	62 ns (9%)	207 ns (91%)	193	0
Ru(bpy) <sub>3</sub> <sup>2+</sup> in Ni(bpy <sub>350</sub> ) <sub>3</sub> •1	93 ns (15%)	305 ns (85%)	273	0.2616
Ru(bpy) <sub>3</sub> <sup>2+</sup> in Ni(bpy <sub>350</sub> ) <sub>3</sub> •2	105 ns (17%)	339 ns (83%)	298	0
Ru(bpz) <sub>3</sub> <sup>2+</sup> in Ni(bpy <sub>350</sub> ) <sub>3</sub> •2	154 ns (12.2%)	851 ns (87.8%)	766	0
Ru(bpz) <sub>3</sub> <sup>2+</sup> in 1(Ni(bpy <sub>350</sub> ) <sub>3</sub> •2) + 0.14(Ni(bpy <sub>350</sub> ) <sub>3</sub> •1)	142 ns (15.2%)	743 ns (84.8%)	652	0.0327
Ru(bpz) <sub>3</sub> <sup>2+</sup> in 1(Ni(bpy <sub>350</sub> ) <sub>3</sub> •2) + 0.6(Ni(bpy <sub>350</sub> ) <sub>3</sub> •1)	119 ns (15.3%)	630 ns (84.7%)	552	0.0981
Ru(bpz) <sub>3</sub> <sup>2+</sup> in 1(Ni(bpy <sub>350</sub> ) <sub>3</sub> •2) + 3(Ni(bpy <sub>350</sub> ) <sub>3</sub> •1)	66 ns (15%)	416 ns (85%)	364	0.1962
Ru(bpz) <sub>3</sub> <sup>2+</sup> in 1(Ni(bpy <sub>350</sub> ) <sub>3</sub> •2) + 7(Ni(bpy <sub>350</sub> ) <sub>3</sub> •1)	35 ns (7.2%)	251 ns (92.8%)	235	0.2289
Ru(bpz) <sub>3</sub> <sup>2+</sup> in Ni(bpy <sub>350</sub> ) <sub>3</sub> •1	22 ns (17.4%)	174 ns (82.6%)	147	0.2616

<sup>a</sup> Ru(L)<sub>3</sub><sup>2+</sup> (L = bpy, bpm, bpz) was incorporated into molten salts as Ru(L)<sub>3</sub>(SO<sub>3</sub>MePEG<sub>350</sub>)<sub>2</sub>. <sup>b</sup> % contribution of each time component determined as  $(a_i\tau_i)/(a_i\tau_i + a_j\tau_j)$ . <sup>c</sup>  $\langle \tau \rangle = \% \tau_f(\tau_f) + \% \tau_s(\tau_s)$ .



guanine and  $\text{Ru}(\text{bpz})_3^{2+}$  (approximately 10 Å),  $\lambda$  is the reorganizational energy, and  $\beta$  gives the effect of tunneling on the electron-transfer rate. A good estimate of the reorganizational energy can be made from the previously measured value for self-exchange in tailed  $\text{Ru}(\text{bpy})_3^{2+}$ -type molten salts, where  $\lambda = 1.2 \text{ eV}$ .<sup>6</sup> Assuming a typical<sup>29</sup> value for  $\beta = 1 \text{ Å}^{-1}$ , this analysis and the rate constant of  $7 \times 10^6 \text{ s}^{-1}$  give an average electron-transfer distance in the melt of 12.5 Å (center-to-center), which is consistent with average distances determined from molecular models of  $\text{Ru}(\text{bpz})_3^{2+}$  and single-stranded DNA (Supporting Information). This value is similar to that derived from early studies using the Perrin model to describe photoinduced electron transfer with small molecule quenchers in rigid glycerol solution.<sup>26</sup>

## Conclusions

In summary, we have developed DNA molten salts containing varying quantities of guanine and wherein small amounts of photoactive metal complexes can be dissolved. Although both  $\text{Ru}(\text{bpm})_3^{2+}$  and  $\text{Ru}(\text{bpz})_3^{2+}$  are quenched by guanine in dilute aqueous solution, only the more oxidizing bpz excited state is quenched in the melt, implying a higher potential for guanine in the melt than in aqueous solution. We ascribe this difference to the lack of a suitable base to accept a proton from the oxidized guanine in the polyether melt. The DNA apparently organizes the small metal complexes along the backbone to produce higher levels of quenching than expected on the basis of the simple concentrations of guanine. This organization produces a linear dependence of the fraction of excited states quenched on the fraction of guanine. The results for the melt where all of the oligonucleotides contain guanine give a rate constant of  $7 \times 10^6 \text{ M}^{-1} \text{ s}^{-1}$  that is consistent with a conventional tunneling parameter ( $\beta$ ), distances derived from simple molecular models of the metal complex and the single-stranded nucleic acid, and an estimate of the reorganizational energy based on authentic measurements in related complexes. These measurements show how the wealth of new information on guanine electron transfer can be used to further understand electron mobility in the novel molten salt films.

**Acknowledgment.** This work was sponsored by the Department of Defense under Contract No. DAMD17-98-1-8224 (H.H.T.) and the Department of Energy (R.W.M.).

**Supporting Information Available:** Stern–Volmer analysis of  $\text{Ru}(\text{bpz})_3^{2+}$  quenching in DNA molten salts, Stern–Volmer analysis of  $\text{Ru}(\text{bpm})_3^{2+}$  quenching in dGMP solution, plots analogous to Figure 4B for the fast and slow time components of the biexponential fits, and molecular models of the metal complex and single-stranded oligonucleotide illustrating the Ru–guanine center-to-center distances. This material is available free of charge via the Internet at <http://pubs.acs.org>.

## References and Notes

- (1) (a) Terrill, R. H.; Murray, R. W. In *Molecular Electronics*; Jortner, J. A., R. M., Eds.; Blackwell Science: Oxford, U.K., 1997. (b) Tour, J. M. *Acc. Chem. Res.* **2000**, *33*, 791–804.
- (2) (a) Abruna, H. D.; Denisevich, P.; Umana, M.; Meyer, T. J.; Murray, R. W. *J. Am. Chem. Soc.* **1981**, *103*, 1. (b) Chen, X.; He, P.; Faulkner, L. R. *J. Electroanal. Chem. Interfacial Electrochem.* **1987**, *222*, 223–242.
- (c) Shaw, B. R.; Haight, G. P., Jr.; Faulkner, L. R. *J. Electroanal. Chem. Interfacial Electrochem.* **1982**, *140*, 147–153. (d) Moss, J. A.; Argazzi, R.; Bignozzi, C. A.; Meyer, T. J. *Inorg. Chem.* **1997**, *36*, 762–763. (e) Gould, S.; Strouse, G. F.; Meyer, T. J.; Sullivan, B. P. *Inorg. Chem.* **1991**, *30*, 2942–2949. (f) Leidner, C. R.; Sullivan, B. P.; Reed, R. A.; White, B. A.; Crimmins, M. T.; Murray, R. W.; Meyer, T. J. *Inorg. Chem.* **1987**, *26*, 882–891. (g) Denisevich, P.; Abruna, H. D.; Leidner, C. R.; Meyer, T. J.; Murray, R. W. *Inorg. Chem.* **1982**, *21*, 2153–2161.
- (3) Chidsey, C. E. D.; Bertozzi, C. R.; Putvinski, T. M.; Muijsce, A. M. *J. Am. Chem. Soc.* **1990**, *112*, 4301–4306.
- (4) (a) Velazquez, C. S.; E., H. J.; Murray, R. W. *J. Am. Chem. Soc.* **1993**, *115*, 7896. (b) Dickinson, E. V.; Williams, M. E.; Hendrickson, S. M.; Masui, H.; Murray, R. W. *J. Am. Chem. Soc.* **1999**, *121*, 613–616.
- (5) Long, J. W.; Velazquez, C. S.; Murray, R. W. *J. Phys. Chem. A* **1996**, *100*, 5492–5499.
- (6) Masui, H.; Murray, R. W. *Inorg. Chem.* **1997**, *36*, 5118.
- (7) Williams, M. E.; Masui, H.; Long, J. W.; Malik, J.; Murray, R. W. *J. Am. Chem. Soc.* **1997**, *119*, 1997–2005.
- (8) (a) Carlin, R. T.; Fuller, J. *NATO Sci. Ser., II: Math., Phys. Chem.* **2002**, *52*, 321–344. (b) Cairns, E. J.; Mamantov, G.; Tischer, R. P.; Vissers, D. R. *Proc. Electrochem. Soc.* **1984**, *84*–2, 284–312. (c) Welton, T. *Chem. Rev. (Washington, D.C.)* **1999**, *99*, 2071–2083.
- (9) (a) Murphy, C. J.; Arkin, M. R.; Jenkins, Y.; Ghatlia, N. D.; Bossmann, S. H.; Turro, N. J.; Barton, J. K. *Science* **1993**, *262*, 1025–1029. (b) Kelley, S. O.; Jackson, N. M.; Hill, M. G.; Barton, J. K. *Angew. Chem., Int. Ed. Engl.* **1999**, *38*, 941–945. (c) Armistead, P. M.; Thorp, H. H. *Anal. Chem.* **2000**, *72*, 3764–3770.
- (10) Armistead, P. M.; Thorp, H. H. *Anal. Chem.* **2001**, *73*, 558–564.
- (11) Leone, A. M.; Weatherly, S. C.; Williams, M. E.; Thorp, H. H.; Murray, R. W. *J. Am. Chem. Soc.* **2001**, *123*, 218–222.
- (12) Longmire, M. L.; Watanabe, M.; Zhang, H.; Wooster, T. T.; Murray, R. W. *Anal. Chem.* **1990**, *62*, 747.
- (13) Sullivan, B. P.; Baumann, J. A.; Meyer, T. J.; Salmon, D. J.; Lehmann, H.; Ludi, A. *J. Am. Chem. Soc.* **1977**, *99*, 7370–7371.
- (14) Rillema, D. P.; Allen, G.; Meyer, T. J.; Conrad, D. *Inorg. Chem.* **1983**, *22*, 1617–1622.
- (15) Crutchley, R. J.; Lever, A. B. P. *J. Am. Chem. Soc.* **1980**, *102*, 7128–7129.
- (16) (a) Weatherly, S. C.; Yang, I. V.; Thorp, H. H. *J. Am. Chem. Soc.* **2001**, *123*, 1236–1237. (b) Saito, I.; Takayama, M.; Sugiyama, H.; Nakatani, K.; Tsuchida, A.; Yamamoto, M. *J. Am. Chem. Soc.* **1995**, *117*, 6406–6405. (c) Lewis, F. D.; Liu, X.; Liu, J.; Hayes, R. T.; Wasielewski, M. R. *J. Am. Chem. Soc.* **2000**, *122*, 12037–12038. (d) Seidel, C. A. M.; Schulz, A.; Sauer, M. H. *J. Phys. Chem.* **1996**, *100*, 5541–5553.
- (17) Steenken, S.; Jovanovic, S. V. *J. Am. Chem. Soc.* **1997**, *119*, 617–618.
- (18) Lafferty, J. J.; Case, F. H. *J. Org. Chem.* **1967**, *32*, 1591–1596.
- (19) Ito, K.; Ohno, H. *Electrochim. Acta* **1998**, *43*, 1247–1252.
- (20) Ritchie, J. E.; Murray, R. W. *J. Phys. Chem. B* **2001**, *105*, 11523–11528.
- (21) Fleming, C. N.; Maxwell, K. A.; DeSimone, J. M.; Meyer, T. J.; Papanikolas, J. M. *J. Am. Chem. Soc.* **2001**, *123*, 10336–10347.
- (22) (a) Lee, E. J.; Wrighton, M. S. *J. Am. Chem. Soc.* **1991**, *113*, 8562–8564. (b) Neshvad, G.; Hoffman, M. Z. *J. Phys. Chem.* **1989**, *93*, 2445–2452. (c) Maidan, R.; Willner, I. *J. Am. Chem. Soc.* **1986**, *108*, 8100–8101. (d) Prasad, D. R.; Hoffman, M. Z. *J. Am. Chem. Soc.* **1986**, *108*, 2568–2573.
- (23) (a) Kumar, C. V.; Barton, J. B.; Turro, N. J. *J. Am. Chem. Soc.* **1985**, *107*, 5518–5523. (b) Orellana, G.; Kirsch-De Mesmaeker, A.; Barton, J. K.; Turro, N. J. *Photochem. Photobiol.* **1991**, *54*, 499–509.
- (24) Based on previously measured values in polyether molten salts.<sup>4–7,11</sup>
- (25) Inokuti, M.; Hirayama, F. *J. Chem. Phys.* **1965**, *43*, 1978–1989.
- (26) (a) Guarr, T.; McGuire, M.; Strauch, S.; McLendon, G. *J. Am. Chem. Soc.* **1983**, *105*, 616–618. (b) Miller, J. R.; Peeples, J. A.; Schmitt, M. J.; Closs, G. L. *J. Am. Chem. Soc.* **1982**, *104*, 6488–6493.
- (27) (a) Turro, N. J. *Modern Molecular Photochemistry*; Benjamin-Cummings: Menlo Park, CA, 1978. (b) Perrin, F. C. *R. Acad. Sci.* **1924**, *178*, 1978–1980.
- (28) Marcus, R. A.; Sutin, N. *Biochim. Biophys. Acta* **1985**, *811*, 265–322.
- (29) (a) Penfield, K. W.; Miller, J. R.; Paddon-Row, M. N.; Cotsaris, E.; Oliver, A. M.; Hush, N. S. *J. Am. Chem. Soc.* **1987**, *109*, 5061–5065. (b) Closs, G. L.; Calcaterra, L. T.; Green, N. J.; Penfield, K. W.; Miller, J. R. *J. Phys. Chem.* **1986**, *90*, 3673–3683. (c) Bixon, M.; Jortner, J. *Adv. Chem. Phys.* **1999**, *106*, 35–202.